Stress Singularities at Tip of a Cutting Tool in Brittle Materials

Makio IINO and Ken KAMINISHI

(Received July 15, 1996)

Abstract

Elastic singularity analyses are performed on the stresses at the tip of a cutting tool with an arbitrary rake angle in a semi-infinite plate of brittle material. On the basis of the formulations developed for the stress analysis at and around the tip of an angled defect, the stresses local to the tip of the cutting tool are derived as functions of the rake angle, and discussed are the effects of alteration in rake angle on the changes in stress distributions, which will determine the nature of surface and subsurface damages of the material generated during machining.

Keywords : Elastic stress singularity, Strength of singularity, Cutting tool, Rake angle, Conformal mapping, Schwartz-Christoffel transformation

1. INTRODUCTION

High strength fine ceramics are facing the problem of surface degradations or failures in the process of machining, because of their very low ductility compared with metallic materials. The high yield strength of ceramic materials are realized at the cost of the low ductility, both the characteristics stemming from their intrinsically high resistance to plastic deformation, which is characteristic of their covalent inter-atomic bonding nature. While there being an engineering importance of developing high strength ceramics with a reasonable ductility at room temperature, machining technology which can control the above-mentioned failures in the presently developed ceramic materials needs to be established.

For the establishment of the machining technology it is essential to know the stress state at and around the tip of the cutting tool in the high strength brittle material concerned, where knowledge will be required of the strength of stress singularities and azimuth dependences of the stresses, which are expected to be importantly influenced by the machining conditions, such as the rake angle, the depth of cut etc.

Because of the room temperature high yield strength and low ductility causing the low machinability of a ceramic material, the seemingly intrinsically poor machinability of the material would be expected to be improved by adoption of a high temperature machining, which would reduce resistance to plastic deformation and improve ductility of the material, and would be realized by a very high speed cutting

Department of Mechanical Engineering, Yamaguchi University 2557 Tokiwadai, Ube, 755 Japan

with very small depth of cut. Actually the possible success of this approarch is suggested by Ueda et al (1991), who experimentally showed a brittle-to-ductile transition in the material removal mode by elevating the cutting speed or by reducing the depth of cut in Si_3N_4 ceramics. They discussed the implications of their experimental results in the light of the numerically calculated path independent integral proposed by Rice and plastic zone area, assuming an initially mode I small crack ahead of the tip of the cutting tool; they do not discuss singular stress fields in works caused by the presence of the tip of the cutting tool itself, which are expected to be influenced by machining parameters, and knowledge of the behavior of which would be important for an understanding of the mechanism of improving the machinability of high strength brittle materials.

In this work the stress analyses will be performed at and around the cutting tool tip, placing emphasis on the strength of elastic stress singularities and azimuth dependences of the stresses, as influenced by the rake angle. The stress analysis, which requires the introduction of a mapping function with singularities of a branch-point type, will be based on the formulations developed in previous work(Iino and Kaminishi, 1996) for the stress analysis at and around the tip of an angled defect.

2. INITIAL FORMULATION

The semi-infinite plate subject to a cutting tool of geometry delineated in Figure 1, with an arbitrary rake angle $\Gamma=\pi/2-\beta$ and a depth of cut c, will be considered, where β denotes the included angle. A rake face is indicated by BO in the figure. The plate lies in the region $Im\ \zeta>0$ of the complex z-plane, $z=x+iy$, with the tip of the cutting tool being located at $z=0$, where $Im\ \zeta$ signifies the imaginary part of an auxiliary complex variable ζ, shown in Figure 2.

For analyses stress functions, $\phi(z)$ and $\chi(z)$, of the complex variable, z, are used; both are arbitrarily chosen analytic functions but satisfy the required boundary conditions, and compose the well-known Airy's function, $F(z)=\mathrm{Re}[\bar{z}\int^{z}dz\phi(z)+$

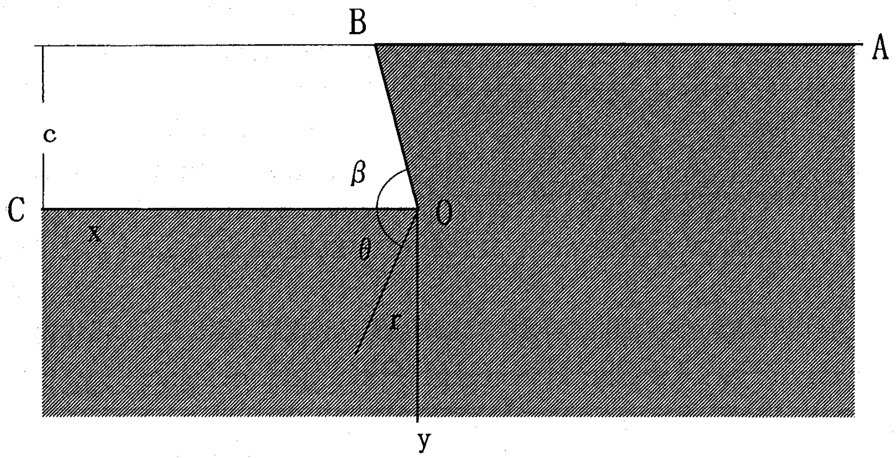

Fig. 1 Semi-infinite plate subject to a cutting tool with an arbitrary rake angle $\Gamma=\pi/2-\beta$

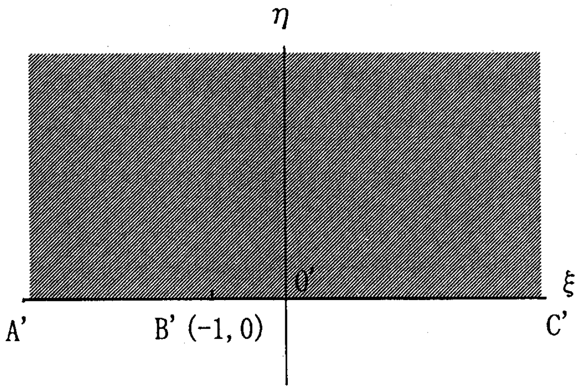

Fig. 2 Auxiliary complex plane, $\zeta=\xi+i\eta$

$\int^z dz \int^z dz \chi(z)]$.

For ease in the boundary condition consideration, an auxiliary complex plane, the ζ-plane, $\zeta=\xi+i\eta$, illustrated in Figure 2, is introduced. The real axis A'B'O'C' and the upper-half of the plane conformally map into the boundary ABOC and the physical region occupied by the plate, shown in Figure 1. This mapping can be attained by application of the Schwartz-Christoffel transformation, the mapping function $\omega(\zeta)$ being found to be of the form

$$z=\omega(\zeta)=A_0+A_1\int_0^\zeta d\zeta\ \zeta^n[\zeta+1]^{-n}, \tag{1}$$

where the exponent, n, is related to β as

$$n=1-\beta/\pi \text{ or } 2\gamma/\pi-1, \tag{2}$$

where $2\gamma=2\pi-\beta$. The constants A_0 and A_1 can be determined as

$$A_0=\omega(0)=0 \text{ and } A_1=c/(2\gamma-\pi), \tag{3}$$

by defining

$$\omega(0)=0 \text{ and } \omega(-1)=ce^{i(2\gamma-\pi)}/\sin 2\gamma. \tag{4}$$

The mapping function, $\omega(\zeta)$, is analytic in the upper-half plane, *Im* $\zeta>0$, but contains singularities describing a cornor point on the boundary, *Im* $\zeta=0$, itself. The cutting tool tip is described by the root of $\omega'(\zeta)=0$, which occurs at $\zeta=0$; from equations(1) to (3) $\omega'(\zeta)$ is given by

$$\omega'(\zeta)=(c/\pi n)\zeta^n[\zeta+1]^{-n}. \tag{5}$$

The prime is meant to denote differentiation by the variable shown in the parentheses, thus $f'(z) = f'(\zeta)/\omega'(\zeta)$. To economize notations we designate $f(z)=f[\omega(\zeta)]$ as $f(\zeta)$. In this way the stresses, σ_ξ, σ_η, $\tau_{\xi\eta}$, and displacements, u_ξ, u_η, in curvilinear coordinates, ξ and η, can be written down as

$$\sigma_\xi+\sigma_\eta=2\phi(\zeta)+\text{ complex conjugate}, \tag{6}$$

$$\sigma_\eta-\sigma_\xi+2i\tau_{\xi\eta}=2\{\omega'(\zeta)/\overline{\omega'(\zeta)}\}\ [\overline{\omega(\zeta)}\{\phi'(\zeta)/\omega'(\zeta)\}+\chi(\zeta)], \tag{7}$$

$$2\mu(u_\xi-iu_\eta)=\{\omega'(\zeta)/|\omega'(\zeta)|\}[\kappa\ \overline{\int^z dz\phi(\zeta)}-\overline{\omega(\zeta)}\phi(\zeta)-\int^z dz\chi(\zeta)\}], \tag{8}$$

where μ is the shear modulus and $\kappa=(3-\nu)/(1+\nu)$, ν being Poisson's ratio(Muskhelishvili, 1963). Bars denote complex conjugates. A more convenient formula for the consideration of boundary conditions can be obtained, by adding equations(6) and (7), as

$$2(\sigma_\eta+i\tau_{\xi\eta})=2\phi(\zeta)+2\overline{\phi(\zeta)}+2\{\omega'(\zeta)/\overline{\omega'(\zeta)}\}[\overline{\omega(\zeta)}\{\phi'(\zeta)/\omega'(\zeta)\}+\chi(\zeta)]. \quad (9)$$

If we let the boundary values of σ_η and $\tau_{\xi\eta}$ at $\eta=0$ and $-1\leqq\xi\leqq 0$ -N(ξ) and- T(ξ), then the boundary conditions on ABOC, Figure 1, can be written in terms of the functions $\phi(\xi)$ and $\chi(\xi)$ as

$$-[N(\xi)+iT(\xi)]\iota(\xi)=\phi(\xi)+\overline{\phi}(\xi)+\{\omega'(\xi)/\overline{\omega}'(\xi)\}[\overline{\omega}(\xi)\{\phi'(\xi)/\omega'(\xi)\}+\chi(\xi)]. \quad (10)$$

$\iota(\xi)$ posseses a value of unity for $-1\leqq\xi\leqq 0$ and vanishes else, and may be expressed by a function

$$\iota(\xi)=(1/\pi)Im[\mathrm{Log}\{\xi/(\xi+1)\}]. \quad (11)$$

Thus, the solution of the problem is attributed to the determination of $\phi(\zeta)$ and $\chi(\zeta)$ which are analytic in $Im\ \zeta>0$ and satisfy the boundary conditions(10). In a domain of interest around the tip of the cutting tool, $|\zeta|<1$, the mapping function $\omega(\zeta)$ can be expressed in a power series as

$$\omega(\zeta)=[c/\pi n(1+n)]\zeta^{1+n}\sum_{k=0}^{\infty}a_k\zeta^k, \quad (12)$$

$$a_0=c_0=1,\ a_k=[(1+n)/(1+n+k)]c_k\ \ (k=1,2,3\cdots) \quad (12a)$$

by term-by-term integration after expansion of equation(5) for $|\zeta|<1$ in a power series. And for large $|\zeta|$, $|\zeta|>1$, as

$$\omega(\zeta)=(c/\pi n)[\zeta-n\mathrm{Log}\zeta-\sum_{k=2}^{\infty}\{c_k/(k-1)\}\zeta^{1-k}], \quad (13)$$

$$c_k=(-1)^k\ n(1+n)\cdots(k-1+n)/k!\ \ (k=1,2,3\cdots) \quad (13a)$$

by term-by-term integration after expansion of equation(5) for $|\zeta|>1$ in a power series.

3. STRESSES AT AND AROUND TIP OF A CUTTING TOOL

In terms of the above developed formulations the essential characters of the stresses, namely cutting-tool-tip singularities and dependences of the stresses on argument θ as influenced by rake angle β, can be disclosed.

Case I N(ξ) and T(ξ) are non-zero constants

Examination of the boundary conditions, equation(10), will suggest that special solutions are given by

$$\phi(\zeta)=0 \text{ and } \chi(\zeta)=-[N_0+iT_0]\iota(\zeta)\overline{\omega'}(\zeta)/\omega'(\zeta), \quad (14)$$

N_0 and T_0 being non-vanishing constants. These yield

$$\sigma_\xi=N_0\iota(\zeta),\ \sigma_\eta=-N_0\iota(\zeta) \text{ and } \tau_{\xi\eta}=-T_0\iota(\zeta), \quad (15)$$

$$u_\xi-iu_\eta=[(N_0+iT_0)/2\pi]\{\omega'(\zeta)/|\omega'(\zeta)|\}\int^{\zeta}d\zeta\overline{\omega'}(\zeta)\iota(\zeta). \quad (16)$$

General solutions will be given by combining the special solutions given above and eigen solutions for the present geometry to be examined below. For determining the general solutions it is assumed that $\phi(\zeta)$ can be represented in a power series as

$$2\phi(\zeta)=2\phi_0(\zeta)+\sum_{k=1}^{\infty}A_k\omega^{\lambda_k-1}(\zeta), \quad (17)$$

and the corresponding $\chi(\zeta)$ is presupposed to be expressed as

$$2\chi(\zeta)=2\chi_0(\zeta)+\sum_{k=1}^{\infty}B_k(\zeta)\omega^{\lambda_k-1}(\zeta), \quad (18)$$

where $\phi_0(\zeta)$ and $\chi_0(\zeta)$ correspond to the special solutions given above, and $\phi(\zeta)$-$\phi_0(\zeta)$ and $\chi(\zeta)$- $\chi_0(\zeta)$ satisfy the condition at $\eta=0$,

$$\phi(\xi)+\overline{\phi}(\xi)+\{\omega'(\xi)/\overline{\omega'}(\xi)\}[\overline{\omega}(\xi)\phi'(\xi)/\omega'(\xi)+\chi(\xi)]=0, \tag{19}$$

For equation(19) to be true for an arbitrary value of ξ, $B_k(\zeta)$ must be of the form

$$B_k(\zeta)=-\overline{\varepsilon_1}(\zeta)[A_k+\overline{A_k}\varepsilon^{\lambda_k-1}(\zeta)]-A_k(\lambda_k-1)\overline{\varepsilon}(\zeta), \tag{20}$$

where $\overline{\varepsilon}(\zeta)=\overline{\omega}(\zeta)/\omega(\zeta)$ and $\overline{\varepsilon_1}(\zeta)=\overline{\omega'}(\zeta)/\omega'(\zeta)$. The bar notation $\overline{f}(\zeta)$ is defined by $\overline{f}(\zeta)=\overline{f(\overline{\zeta})}$. In the above equations(17), (18) and (20) λ_k is assumed to be a positive real number, $\lambda_k>0$, in order for the stresses to be allowed to be singular but for the displacements to be bounded at the tip, $\zeta=0$.

On the real axis OC, $\xi\geqq0$, $\overline{\varepsilon}(\xi)=\overline{\varepsilon_1}(\xi)=1$, where from equation(20)

$$B_k(\xi)=-A_k\lambda_k-\overline{A_k} \qquad (\xi\geqq0). \tag{21}$$

Thus, $B_k(\zeta)$ is a set of oonstants on the real axis OC. On BO, $-1\leqq\xi\leqq0$, $\overline{\varepsilon}(\xi)=e^{\pm i2\pi(1+n)}=e^{\pm i4\gamma}$ and $\overline{\varepsilon_1}(\xi)=e^{\pm i2\pi n}=e^{\pm i2(2\gamma-\pi)}=e^{\pm i4\gamma}$, where from equation(20)

$$B_k(\xi)=-A_k\lambda_k e^{\pm i4\gamma}-\overline{A_k}e^{\pm i\lambda_k 4\gamma} \quad (-1\leqq\xi\leqq0) \tag{22}$$

must hold. Thus $B_k(\zeta)$ on BO must be another set of constants. Equating both the constants reduces to

$$\begin{bmatrix} 1-\cos\lambda_k 2\gamma+\lambda_k(1-\cos4\gamma) & \pm(\sin\lambda_k 4\gamma-\lambda_k\sin4\gamma) \\ \pm(\sin\lambda_k 4\gamma-\lambda_k\sin4\gamma) & 1-\cos\lambda_k 2\gamma+\lambda_k(1-\cos4\gamma) \end{bmatrix} \begin{bmatrix} Re A_k \\ Im A_k \end{bmatrix} = \begin{bmatrix} 0 \\ 0 \end{bmatrix} \tag{23}$$

For a non-zero value of A_k to be ensured the determinant of the coefficients must vanish, i.e.,

$$\lambda_k^2\sin^2 2\gamma -\sin^2\lambda_k 2\gamma=0. \tag{24}$$

Thus, λ_k is found the eigen solution of

$$\lambda_k\sin2\gamma +\sin\lambda_k 2\gamma=0, \tag{24a}$$

or

$$\lambda_k\sin2\gamma -\sin\lambda_k 2\gamma=0. \tag{24b}$$

The former corresoponds to deformation of symmetric mode, and the latter of skew-symmetric mode with respect to an angle $\theta=\gamma$; in the mixed mode deformation under consideration solutions for both the modes should be superimposed. For the present geometry coefficients A_k are arbitrary, coefficients $B_k(\zeta)$ being related to A by equation(21), (22) or (26) to appear below.

On AB, on the other hand, it is found that $B_k(\zeta)$ could not be constant, because $\overline{\varepsilon}(\xi)$ varies although $\overline{\varepsilon_1}(\xi)$ keeps constant there, $\overline{\varepsilon_1}(\xi)=1$, Since $\overline{\varepsilon}(\xi)$ can be expressed rather simply by a function of θ as †

$$\begin{aligned}\overline{\varepsilon}(\xi)&=(x+ic)/(x-ic)=-(c^2-x^2-i2cx)/(c^2+x^2)\\&=-\exp[i\tan^{-1}\{-2cx/(c^2-x^2)\}]=-\exp[i\tan^{-1}\{-\tan(2\theta-3\pi)\}]\\&=e^{-i2\theta},\end{aligned} \tag{25}$$

$B_k(\zeta)$ on AB turns out to be a function of a single variable, θ.

$$B_k(\xi)=-A_k\{1+(\lambda_k-1)e^{-i2\theta}\}-\overline{A_k}e^{-i(\lambda_k-1)2\theta} \quad (\xi\leqq-1). \tag{26}$$

In the complex ζ plane, where $\omega(\zeta)$ is expanded as in equation(12) or (13) depending on the ζ area, it is understood that $B_k(\zeta)$ can be expressed as

$$\begin{aligned}B_k(\zeta)&=-A_k\lambda_k e^{\pm i4\gamma}-\overline{A_k}e^{\pm i\lambda_k 4\gamma}\\&=-A_k\lambda_k-\overline{A_k} \qquad (|\zeta|\leqq1),\end{aligned} \tag{27}$$

† Note that $x/c = \tan(\theta-3\pi/2)$ in the derivation of equation(25).

and

$$B_k(\zeta) = -A_k[1+(\lambda_k-1)\overline{\varepsilon}(\zeta)] - \overline{A_k}\varepsilon^{\lambda_k-1}(\zeta) \qquad (|\zeta|>1). \tag{28}$$

Among terms in an infinite series indicated in equations(17) and (18) the most important term at the cutting tool tip is the dominantly singular term corresponding to the minimum real root, λ_1, of the eigen equation(24a) or (24b); the quantity $1-\lambda_1$ determines the strength of the first singularity, as will be described below. The stresses in polar coordinates, r and θ, illustrated in Figure 1, of the dominant singularities can be obtained from the relations,

$$\sigma_r + \sigma_\theta = 2[\phi(\zeta) + \overline{\phi(\zeta)}], \tag{29}$$

$$\sigma_\theta - \sigma_r + 2i\tau_{r\theta} = 2e^{i2\theta}[\overline{\omega(\zeta)}\{\phi'(\zeta)/\omega'(\zeta)\} + \chi(\zeta)], \tag{30}$$

with $2\phi(\zeta) = A_1\omega^{\lambda_1-1}(\xi)$, $2\chi(\zeta) = B_1\omega^{\lambda_1-1}(\xi)$, and $B_1 = -A_1\lambda_1 - \overline{A_1}$ from equation(27). They are

$$\sigma_r = |A_1|\, r^{-(1-\lambda)}[\cos(1-\lambda)\theta_1 + \cos(\theta_1+\lambda\gamma)\cos(\lambda\theta) - \lambda\sin\theta\sin(\lambda\theta_1+\gamma)], \tag{31}$$

$$\sigma_\theta = |A_1|\, r^{-(1-\lambda)}[\cos(1-\lambda)\theta_1 - \cos(\theta_1+\lambda\gamma)\cos(\lambda\theta) + \lambda\sin\theta\sin(\lambda\theta_1+\gamma)], \tag{32}$$

$$\sigma_{r\theta} = |A_1|\, r^{-(1-\lambda)}[-\cos(\theta_1+\lambda\gamma)\sin(\lambda\theta) - \lambda\sin\theta\cos(\lambda\theta_1+\gamma)], \tag{33}$$

with $\lambda = \lambda_1$, the smallest root of equation(24a) for symmetric mode. And

$$\sigma_r = |A_1|\, r^{-(1-\lambda)}[\sin(1-\lambda)\theta_1 + \sin(\theta_1+\lambda\gamma)\cos(\lambda\theta) - \lambda\sin\theta\cos(\lambda\theta_1+\gamma)], \tag{34}$$

$$\sigma_\theta = |A_1|\, r^{-(1-\lambda)}[\sin(1-\lambda)\theta_1 - \sin(\theta_1+\lambda\gamma)\cos(\lambda\theta) + \lambda\sin\theta\cos(\lambda\theta_1+\gamma)], \tag{35}$$

$$\sigma_{r\theta} = |A_1|\, r^{-(1-\lambda)}[-\sin(\theta_1+\lambda\gamma)\sin(\lambda\theta) + \lambda\sin\theta\sin(\lambda\theta_1+\gamma)], \tag{36}$$

with $\lambda = \lambda_1$, the smallest root of equation(24b) for skew-symmetric mode. In equations (31) to (36) $\theta_1 = \theta - \gamma$.

Case II N(ξ)and T(ξ) varies as $|\omega(\xi)|^{-\varkappa}$

It is assumed that N(ξ) and T(ξ) varies as $|\omega(\xi)|^{-\varkappa}$. Here $\varkappa$ is assumed to be a real number satisfying $0<\varkappa<1$ for the stresses to be allowed to be singular but the displacements to be bounded at the tip of the cutting tool. In this case it can be assumed that $\phi(\zeta)$ and $\chi(\zeta)$ depend on $\omega(\zeta)$ as

$$2\phi(\zeta) = C\omega^{-\varkappa}(\zeta), \tag{37}$$

$$2\chi(\zeta) = D(\zeta)\omega^{-\varkappa}(\zeta). \tag{38}$$

The boudary conditions on ABOC, $\eta=0$, equation(10), are described now by

$$-2[N_1+iT_1]\omega^{-\varkappa}(\xi)e^{\mp i\varkappa 2\gamma}\iota(\xi)$$
$$= C\omega^{-\varkappa}(\xi) + \bar{C}\bar{\omega}^{-\varkappa}(\xi) + \varepsilon_1(\xi)[-C\varkappa\bar{\omega}(\xi)\omega^{-1-\varkappa}(\xi) + D(\xi)\omega^{-\varkappa}(\xi)], \tag{39}$$

where it is first assumed that on BO N(ξ) and T(ξ) varies as

$$N(\xi)+iT(\xi) = [N_1+iT_1]\,|\omega(\xi)|^{-\varkappa} = [N_1+iT_1]\omega^{-\varkappa}(\xi)e^{\mp i\varkappa 2\gamma}; \tag{40}$$

it is to be noted on BO $\omega(\xi) = |\omega(\xi)|e^{\mp i2\gamma}$, therefore $|\omega(\xi)| = \omega(\xi)e^{\pm i2\gamma}$.

Similar reasonings which lead to equations(21) and (22) yield the relation

$$D(\xi) = -C(1-\varkappa) - \bar{C} \qquad (\xi \geqq 0), \tag{41}$$

$$D(\xi) = -C(1-\varkappa)e^{\pm i4\gamma} - \bar{C}e^{\pm i(1-\varkappa)4\gamma} - 2(N_1+iT_1)e^{\pm i(2-\varkappa)2\gamma} \quad (-1 \leqq \xi \leqq 0). \tag{42}$$

Thus, D(ζ) on BO, $-1\leqq\xi\leqq0$, and OC, $\xi\geqq 0$, are found to be a and another constants. Equating both the constants reduces to

$$\begin{bmatrix} (1-\varkappa)\sin2\gamma\cos(1-\varkappa)2\gamma + \cos2\gamma\sin(1-\varkappa)2\gamma & \mp\varkappa\sin2\gamma\sin(1-\varkappa)2\gamma \\ \mp(2-\varkappa)\sin2\gamma\sin(1-\varkappa)2\gamma & (1-\varkappa)\sin2\gamma\cos(1-\varkappa)2\gamma - \cos2\gamma\sin(1-\varkappa)2\gamma \end{bmatrix} \begin{bmatrix} Re\,C \\ Im\,C \end{bmatrix}$$

$$= \begin{bmatrix} T_1 \\ -N_1 \end{bmatrix} \tag{43}$$

Then C can be determined as

$$C = (-i/\Delta)\left[(1-\varkappa)e^{-i(1-\varkappa)2\gamma}\sin 2\gamma\{N_1+iT_1\}+e^{i2\gamma}\sin(1-\varkappa)2\gamma\{N_1-iT_1\}\right], \quad (44)$$

or

*Re*C

$$= (-1/\Delta)\left[(1-\varkappa)\sin 2\gamma\{N_1\sin(1-\varkappa)2\gamma-T_1\cos(1-\varkappa)2\gamma\}-\sin(1-\varkappa)2\gamma\{N_1\sin 2\gamma-T_1\cos 2\gamma\}\right], \quad (44a)$$

*Im*C

$$= (-1/\Delta)\left[(1-\varkappa)\sin 2\gamma\{N_1\cos(1-\varkappa)2\gamma+T_1\sin(1-\varkappa)2\gamma\}+\sin(1-\varkappa)2\gamma\{N_1\cos 2\gamma+T_1\sin 2\gamma\}\right], \quad (44b)$$

where

$$\Delta = (1-\varkappa)^2\sin^2 2\gamma-\sin^2(1-\varkappa)2\gamma, \quad (45)$$

the determinant of the coefficient matrix in equation(43), which must not vanish for C to be finite. Further, by similar reasonings which lead to equations(27) and (28), D(ζ) is found to be related to C as

$$D(\zeta) = -C(1-\varkappa)-\bar{C} \qquad (|\zeta|\leqq 1), \quad (47)$$

and

$$D(\zeta) = -C[1-\varkappa\bar{\varepsilon}(\zeta)]-\bar{C}\bar{\varepsilon}^{-\varkappa}(\zeta) \qquad (|\zeta|>1). \quad (48)$$

For a little more arbitrary boundary conditions on BC, which can be of greater practical importance,

$$P(\xi) = -N(\xi)-iT(\xi) = [-N_1|\omega(\xi)|^{-\varkappa_1}-iT_1|\omega(\xi)|^{-\varkappa_2}], \quad (49)$$

the solutions can be obtained by superimposing those under the boundary conditions

$$P(\xi) = P_1(\xi) = -N_1|\omega(\xi)|^{-\varkappa_1}\iota(\xi), \quad (50)$$

and those under the boundary conditions

$$P(\xi) = P_2(\xi) = -iT_1|\omega(\xi)|^{-\varkappa_2}\iota(\xi). \quad (51)$$

For boundary conditions $P(\xi)=P_1(\xi)$, C and D(ζ) are determined as

$$C = C_1 = (-iN_1/\Delta)\left[(1-\varkappa_1)e^{-i(1-\varkappa_1)2\gamma}\sin 2\gamma+e^{i2\gamma}\sin(1-\varkappa_1)2\gamma\right], \quad (50a)$$

$$D(\zeta) = D_1 = (-iN_1/\Delta)\left[(1-\varkappa_1)\{e^{i(1-\varkappa_1)2\gamma}-(1-\varkappa_1)e^{-i(1-\varkappa_1)2\gamma}\}\sin 2\gamma + \{e^{-i2\gamma}-(1-\varkappa_1)e^{i2\gamma}\}\sin(1-\varkappa_1)2\gamma\right] \qquad (|\zeta|\leqq 1), \quad (50b)$$

D(ζ) for $|\zeta|>1$ being related to C_1 as $D(\zeta)=-C_1[1-\varkappa_1\bar{\varepsilon}(\zeta)]-\bar{C}_1\bar{\varepsilon}^{-\varkappa_1}(\zeta)$ $(|\zeta|>1)$, and for boundary conditions $P_2(\xi)$, as

$$C = C_2 = (-T_1/\Delta)\left[-(1-\varkappa_2)e^{-i(1-\varkappa_2)2\gamma}\sin 2\gamma+e^{i2\gamma}\sin(1-\varkappa_2)2\gamma\right], \quad (51a)$$

$$D(\zeta) = D_2 = (-T_1/\Delta)\left[(1-\varkappa_2)\{e^{i(1-\varkappa_2)2\gamma}+(1-\varkappa_2)e^{-i(1-\varkappa_2)2\gamma}\}\sin 2\gamma - \{e^{-i2\gamma}+(1-\varkappa_2)e^{i2\gamma}\}\sin(1-\varkappa_2)2\gamma\right] \qquad (|\zeta|\leqq 1), \quad (51b)$$

D(ζ) for $|\zeta|>1$ being related to C_2 as $D(\zeta)=-C_2[1-\varkappa_2\bar{\varepsilon}(\zeta)]-\bar{C}_2\bar{\varepsilon}^{-\varkappa_2}(\zeta)$ $(|\zeta|>1)$. Thus, the problem is solved. For instance, for boundary conditions $P(\xi) = P_1(\xi)$ the stresses in polar cordinates, r and θ, at the root of the tool tip are given, after algebraic manipulations, as

$$\sigma_r = (N/\Delta)r^{-\varkappa}[\{\varkappa\sin 2\gamma\sin\{(1-\varkappa)2\gamma\}\{2\cos\theta\cos(1-\varkappa)\theta+\varkappa\sin\theta\sin(1-\varkappa)\theta\} + \{(1-\varkappa)\sin 2\gamma\cos(1-\varkappa)\gamma+\cos 2\gamma\sin(1-\varkappa)2\gamma\}\{\cos\theta\sin(1-\varkappa)\theta-(1+\varkappa)\sin\theta\cos(1-\varkappa)\theta\}], \quad (52)$$

$$\sigma_\theta = (N/\Delta)r^{-\varkappa}[\varkappa(2-\varkappa)\sin 2\gamma\sin\{(1-\varkappa)2\gamma\sin\theta\sin(1-\varkappa)\theta - \{(1-\varkappa)\sin 2\gamma\cos(1-\varkappa)2\gamma+\cos 2\gamma\sin(1-\varkappa)2\gamma\}\{(1-\varkappa)\sin\theta\cos(1-\varkappa)\theta-\cos\theta\sin(1-\varkappa)\theta\}], \quad (53)$$

$$\tau_{r\theta} = (N/\Delta)r^{-\varkappa}\varkappa[-\sin 2\gamma\sin\{(1-\varkappa)2\gamma\{(1-\varkappa)\sin\theta\cos(1-\varkappa)\theta+\cos\theta\sin(1-\varkappa)\theta\} + \{(1-\varkappa)\sin 2\gamma\cos(1-\varkappa)2\gamma+\cos 2\gamma\sin(1-\varkappa)2\gamma\}\sin\theta\sin(1-\varkappa)\theta], \quad (54)$$

with $\varkappa=\varkappa_1$ and $\Delta=(1-\varkappa)^2\sin^2 2\gamma-\sin^2(1-\varkappa)2\gamma$, equation(45).

The influence of a rake angle on these stresses, with $\varkappa$ being assumed to be 0.46, are demonstrated in Figures 3, 4 and 5, which show how negative increase in the rake angle causes a significant decrease in the maximum amplitude of singularity especially in normal stresses, σ_θ and σ_r, thus leveling off the stress fields. In Figures 3 and 4, you can see that a stress state in which the peak normal stress, σ_θ, and the zero shear stress, $\tau_{r\theta}$, coincidently take place at approximately 135° for zero rake angle, is greately changed when rake angle is altered to minus 15°, for which the peak normal stress, σ_θ, is reduced to one tenth for the assumed $\varkappa$ value, the angle at which the reduced peak stress takes place being shifted to approximately 120°; the two maximal shear stresses, $\tau_{r\theta}$, positive ang negative, also are reduced but to smaller degrees, with change in

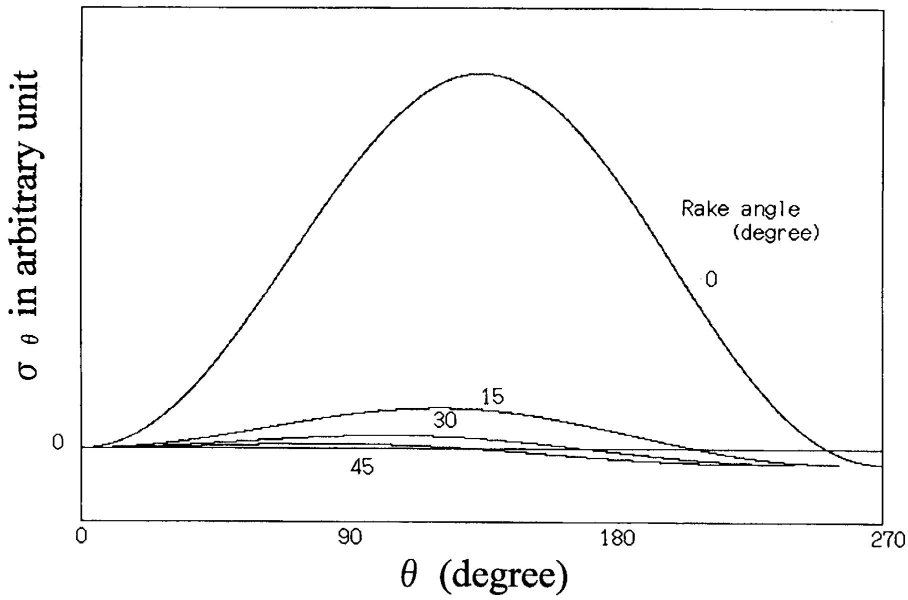

Fig. 3 Influence of rake angle on σ_θ as a function of θ

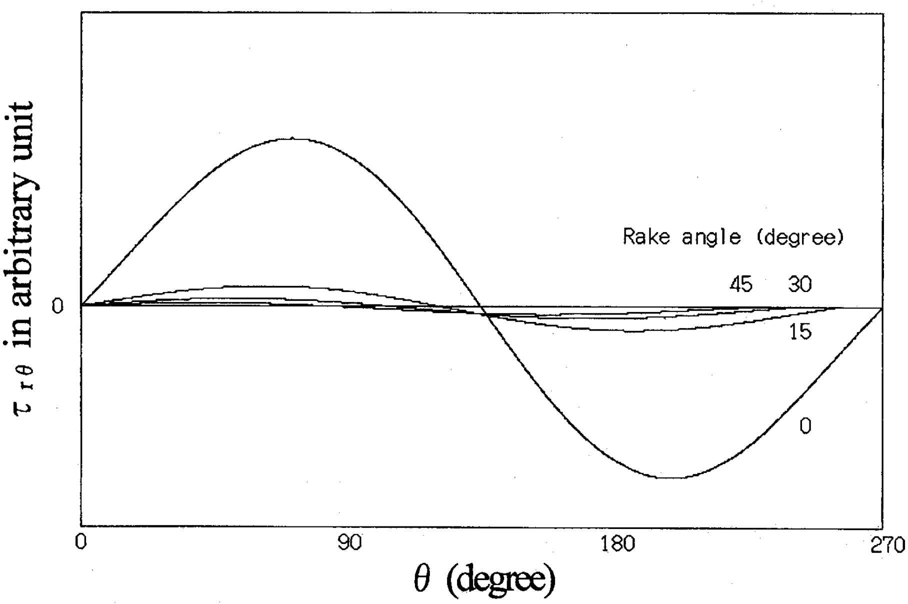

Fig. 4 Influence of rake angle on $\tau_{r\theta}$ as a function of θ

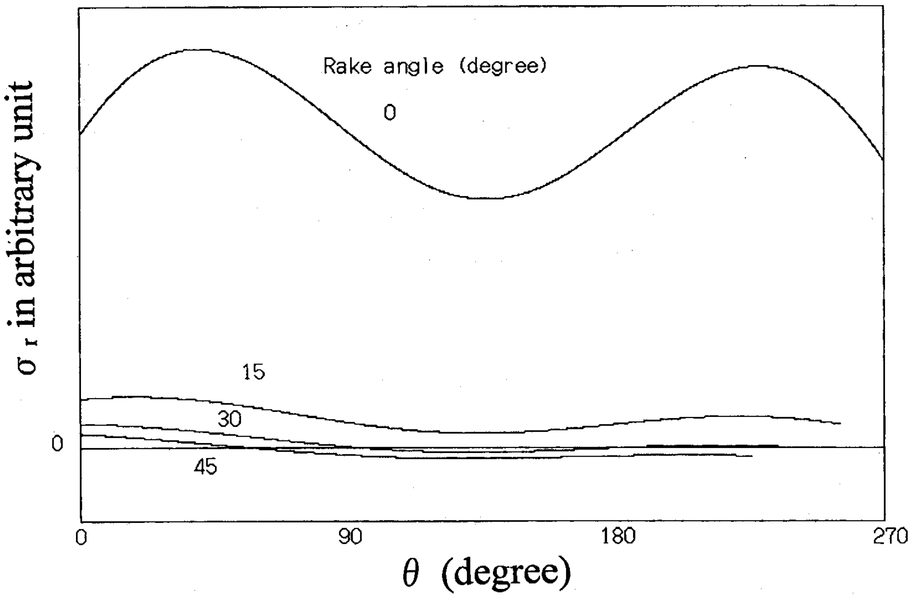

Fig. 5 Influence of rake angle on σ_r as a function of θ

angles of the occurrence from 70°and 200°to 60°and 185°. These behaviors would suggest that the alteration in rake angle may possibly accelerate shear stress-induced plastic deformation and other faultings rather than normal stress-induced crackings, which implies a change in the nature of surface and subsurface damages of the material generated during machining. Figure 5 shows that the peak radial stress, σ_r, is again greatly reduced upon change in rake angle of zero to minus 15°. Further, a change in rake angle from zero to minus 45°substantially smoothes out the singular stress fields, both normal and shear, as seen from Figures 3 to 5.

It is acknowledged that the above described boundary counditions, *Case I* and *Case II*, are elementary and assumptive, since there seem to be neither experimental nor theoretical discussions on the validity of the assumptions for the distribution of tractions on the rake face in works of ceramic materials. Shirai (1990) has given computational predictions for the normal and shear stress, $-N(\xi)$ and $-T(\xi)$, on the rake face in works of Inconel, X-750, and carbon steel, S45C, which show that the normal stress, $-N(\xi)$, should depend on $\omega(\xi)$ following approximately the inverse power law, but vanishing at a distance of several times the depth of cut, and $-T(\xi)$ should keep approximately constant for some distance from the origin, $\xi=0$, again decaying to vanish at approximately the same distance as with $-N(\xi)$. Thus, so far as the metals and alloys are concerned, the boundary conditions seem to be governed neither simply by the constant nor by the inverse power law, yet it is expected that the above mentioned discussions for *Case I* and *Case II* will cast a new light on the understanding of the singular stress distributions at and around the tip of the cutting tool as influenced by a rake angle.

4. CONCLUSIONS

On the basis of the formulations developed for the stress analysis at and around the tip of an angled defect, the stresses local to the tip of the cutting tool are derived as functions of a rake angle, and discussed are the effects of alteration in the rake angle on the changes in the normal and shear stress distributions in the vicinity of the tool tip, which are expected to determine the nature of surface and subsurface damages of the material generated during machining.

5. REFERENCES

Muskhelishvili, N.I. (1963) Some Basic Problems of the Mathematical Theory of Elasticity, pp. 171-190, P. Noordhoff Ltd., Groningen-the Netherlands, 1963.

Shirai, E. (1990) Modern Theory of Metal Cutting(現代切削理論), pp. 342-344, Kyoritsu Shuppan Co. Ltd., 1990 (in Japanese).

Ueda, K., Sugita, T and Hiraga, H. (19911) Annals of the CIRP, Vol. 40-1, pp. 61-64, 1991.

Iino, M. and Kaminishi, K. (1996), This volume.